Enhanced expression of potassium-chloride cotransporter KCC2 in human temporal lobe epilepsy

Mária R. Karlócai[1], Lucia Wittner[1.2,3], Kinga Tóth[1.2], Zsófia Maglóczky[1], Zoja Katarova[1], György Rásonyi[3], Loránd Erőss[3,] Sándor Czirják[3], Péter Halász[3], Gábor Szabó[1], John A. Payne[4], Kai Kaila[5], Tamás F. Freund[1*]

[1]Inst. Experimental Medicine, Hungarian Acad. Sci., Budapest, Hungary, [2]Institute of Cognitive Neuroscience and Psychology, Research Institute of Natural Sciences, Hungarian Acad. .Sci., H-1117 Budapest, Hungary, [3]National Institute of Clinical Neuroscience, Budapest, H-1577, [4]Dept. Physiology and Membrane Biology, School of Medicine, Univ. California, Davis, CA 95616, [5]Department of Biosciences, University of Helsinki, FIN-00014, Helsinki, Finland

Corresponding author: Mária R. Karlócai, address: Szigony 43, Budapest, 1083, Hungary; e-mail: karlocai.rita@mta.koki.hu; telephone: +36-1-210-9400, fax: +36-1-210-9412

Abstract

Synaptic reorganization in the epileptic hippocampus involves altered excitatory and inhibitory transmission besides the rearrangement of dendritic spines, resulting in altered excitability, ion homeostasis, and cell swelling. The potassium-chloride cotransporter-2 (KCC2) is the main chloride extruder in neurons and hence will play a prominent role in determining the polarity of $GABA_A$ receptor-mediated chloride currents. In addition, KCC2 also interacts with the actin cytoskeleton which is critical for dendritic spine morphogenesis, and for the maintenance of glutamatergic synapses and cell volume.

Using immunocytochemistry, we examined the cellular and subcellular levels of KCC2 in surgically removed hippocampi of temporal lobe epilepsy (TLE) patients and compared them to control human tissue. We also studied the distribution of KCC2 in a pilocarpine mouse model of epilepsy. An overall increase in KCC2-expression was found in epilepsy and confirmed by Western blots. The cellular and subcellular distributions in control mouse and human samples were largely similar; moreover, changes affecting KCC2-expression were also alike in chronic epileptic human and mouse hippocampi.

At the subcellular level, we determined the neuronal elements exhibiting enhanced KCC2 expression. In epileptic tissue, staining became more intense in the immunopositive elements detected in control tissue, and profiles with subthreshold expression of KCC2 in control samples became labelled. Positive interneuron somata and dendrites were more numerous in epileptic hippocampi, despite severe interneuron loss.

Whether the elevation of KCC2-expression is ultimately a pro- or anticonvulsive change, or both - behaving differently during ictal and interictal states in a context-dependent manner - remains to be established.

Keywords: GABA, spinogenesis, human TLE, KCC2, hippocampus

Abbreviations: CA = cornu Ammonis; DAB = 3,3‘diamino-benzidine 4 HCl; DG = dentate gyrus; EEG= electroencephalogram; GABA = gamma-aminobutyric acid; GluR1 = Glutamate receptor 1; KCC2 = Potassium-chloride cotransporter-2; PET = positron emission tomography;

pilo = pilocarpine; SE = status epilepticus; str = stratum; SPECT = single-photon emission computerized tomography; TLE = temporal lobe epilepsy

Introduction

Members of the potassium-chloride cotransporter (KCC) family are known to play important roles in cellular ion and water homeostasis (Hoffmann and Dunham, 1995; Lang et al., 1998). In addition, they are involved in dendritic spinogenesis (Fiumelli et al., 2013; Li et al., 2007) . The potassium-chloride cotransporter-2 (KCC2) acts as a crucial ion-transport system in neurons (Payne et al., 1996; Payne, 1997; Rivera et al., 1999). By maintaining low intracellular [Cl^-], KCC2 is essential for fast hyperpolarizing $GABA_A$ receptor-mediated inhibition (Kaila et al., 2014a).

Temporal lobe epilepsy (TLE) is frequently associated with hippocampal pathology (Corsellis, 1955; Green, 1991; Margerison and Corsellis, 1966). The main pathological changes in the hippocampus are cell loss and synaptic reorganization, but the pattern and degree of changes are variable (Blackwood and Corsellis, 1976; Corsellis, 1955; de Lanerolle et al., 2003; Green, 1991; Mathern et al., 1997a; McNamara, 1999). The vulnerability of principal cells (pyramidal cells of the CA1 region and endfolium) has been studied in hippocampal sclerosis and was found to be the most frequent morphological change in the brain of patients with chronic temporal lobe epilepsy (Corsellis, 1955; Green, 1991; Magloczky, 2010; Margerison and Corsellis, 1966), together with a loss of specific interneuron types (de Lanerolle et al., 1989; Magloczky et al., 2000; Robbins et al., 1991; Sloviter, 1987; Toth et al., 2010; Wittner et al., 2001; Zhang et al., 2009; Zhu et al., 1997).

Due to the loss of certain interneurons, impairment of GABAergic inhibition was often proposed to be the main cause of epileptic seizure generation (Colder et al., 1996; Sloviter, 1987). However, morphological (Babb et al., 1989; Wittner et al., 2001) and physiological (Cossart et al., 2001; Mody et al., 1995; Wilson et al., 1998; Wilson, 1999; Ylinen et al., 1991) data have supported the preservation of perisomatic inhibition in epileptic tissue and have shown a selective impairment of dendritic inhibition (Cossart et al., 2001).

Several features of excitation become altered in chronic epilepsy, such as the sprouting of excitatory fibres (Buckmaster and Dudek, 1997; Laurberg and Zimmer, 1981; Sutula et al., 1989), the alteration of postsynaptic AMPA and NMDA receptors (Mathern et al., 1997b; Mathern et al., 1998), or the rearrangement of dendritic spines (Isokawa, 2000; Swann et al., 2000). Since KCC2 is known to have a role in dendritic spinogenesis and the aggregation of postsynaptic GluR1-containing AMPA receptors (Fiumelli et al., 2013; Gauvain et al., 2011), a change in KCC2 level could easily lead to drastic changes in the excitability of the neuronal network.

Moreover, an increasing number of studies have shown that impaired chloride homeostasis may lead to a depolarizing effect of GABA (Kaila et al., 1997; Kaila et al., 2014a; Kaila et al., 2014b; Smirnov et al., 1999; Viitanen et al., 2010). GABAergic transmission has been shown to become excitatory in a minority of principal neurons of the epileptic human temporal lobe (Cohen et al., 2002; Huberfeld et al., 2007), as well as in animal models (Fujiwara-Tsukamoto et al., 2003; Stein and Nicoll, 2003). This may be due to a decrease in KCC2 expression in vulnerable regions or cell types; to bicarbonate-driven Cl^- accumulation and consequent elevation of interstitial K^+ which can lead to an apparently paradoxical, excitatory mode of GABAergic transmission (Viitanen et al., 2010); or due to altered potassium homeostasis caused by e.g. the ineffective uptake of extracellular potassium by astrocytes (Heinemann et al., 2000; Stewart et al., 2010). Thus, the expression of this protein may also be involved in the regulation of neuronal volume changes. It is important to note that KCC2 was shown to be expressed mostly in the vicinity of excitatory synapses (Gulyas et al., 2001).

Although several earlier studies have dealt with the nature of changes affecting KCC2 (Galanopoulou, 2008; Jaenisch et al., 2010; Okabe et al., 2003; Papp et al., 2008; Puskarjov et al., 2012; Rivera et al., 1999) its subcellular distribution in human hippocampus is unknown, and consequently, anatomical alterations of KCC2 expression have never been compared between early post-mortem human TLE patients and controls at the electron microscopic level. In this study, we took advantage of the unique opportunity to investigate differences in KCC2 expression in TLE and human control tissue. Importantly, one should take into account that the postmortem delay of control human tissue may modify the immunoreactions, therefore we also investigated the distribution of KCC2 in an animal model of chronic epilepsy (Karlocai et al., 2011). Quantitative changes were studied using Western blots. To uncover any changes in the

pattern of KCC2 expression in epilepsy, immunohistochemistry was carried out followed by light and electron microscopic examination in the chronic phase (both mice and humans).

Experimental procedures

Human samples

KCC2-containing elements were examined in the hippocampi of 12 human control samples and in 32 temporal lobe samples surgically removed from epileptic patients. Patients with intractable temporal lobe epilepsy underwent surgery at the National Institute of Clinical Neuroscience, Budapest, within the framework of the "Hungarian Epilepsy Surgery Program". Standard anterior temporal lobectomies were performed (Spencer and Spencer, 1985), i.e. the anterior third of the temporal lobe was removed together with the temporomedial structures. Samples from patient with lesions other than hippocampal sclerosis were not used. Control brain samples were obtained from human subjects (37-72 years old), none of whom had a record of any neurological disorders. Brains were removed 2-4 hours after death; the autopsy was performed in the Department of Forensic Medicine of the Semmelweis University Medical School, Budapest. Harvesting of tissues was approved by the local ethics committee, and informed consent was obtained from the next of kin. Tissue was obtained and used in accordance with the Declaration of Helsinki. All procedures were approved by the Regional and Institutional Committee of Science and Research Ethics of Scientific Council of Health (TUKEB 5-1/1996).

In four out of 12 autopsy control hippocampal samples and 18 of the epileptic samples, a part of the resected tissue was separated and snap frozen immediately for further Western blot analysis. The remaining part of the 18 epileptic samples and further 14 epileptic hippocampal samples were dissected into 3-4 mm thick blocks, and immersed into a fixative containing 4% paraformaldehyde, 0.05% glutaraldehyde and 0.2% picric acid in 0.1 M phosphate buffer (PB, pH=7,4). The fixative was changed every 30 min to a fresh solution during constant agitation for 6 hours, and then the blocks were postfixed in the same fixative overnight without glutaraldehyde. Another 6 control hippocampi (post mortem delay 2-4 hours) were subjected to the same procedure. The remaining two control brains (control numbers 10 and 11) were removed from the skull 2 hours after death, both internal carotid and vertebral arteries were

cannulated, and the brains were perfused first with physiological saline (2 liters in 30 minutes) followed by a fixative solution containing 0.05% glutarealdehyde, 4% paraformaldehyde and 0.2% picric acid in 0.1 M PB (6 liters in 1,5 hour). The hippocampus was removed after perfusion and cut into 3-4 mm thick blocks, which were postfixed in the same fixative solution without glutarealdehyde overnight.

Animal model of epilepsy

For the animal model of TLE, 66 CD1 (p25-p37) male mice (Harlan, Italy) were used and 47 were treated with pilocarpine. Animals were kept under standard conditions with a 12 h dark-light cycle; food and water were supplied *ad libitum*. Experiments were performed according to the guidelines of the Institutional Ethical Codex & the Hungarian Act of Animal Care & Experimentation (1998, XXVIII, Section 243/1998). The Animal Care and Experimentation Committee of the Institute of Experimental Medicine of Hungarian Academy of Sciences and the Animal Health and Food Control Station, Budapest, approved the experimental design under the directive 2303/003/FŐV/2006. The experiments are in accordance with 86/609/EEC/2 Directives of the European Community, which is in full agreement with the regulation of animal experiments in the European Union. Animals were randomly assigned to control and experimental groups. Age-matched control mice (n=19) were injected with physiological saline or scopolamine, whereas experimental mice were injected with intraperitoneal Pilocarpine hydrochloride (340 mg/kg, Sigma-Aldrich, USA) to induce status epilepticus (SE). Scopolamine methyl nitrate (5 mg/kg, Sigma-Aldrich, USA) was injected 30 minutes in advance to prevent the peripheral cholinergic effects of pilocarpine (Karlocai et al., 2011; Magloczky et al., 2010).

For further details see (Karlocai et al., 2011) and *Supplementary experimental procedures*.

In the present study animals were sacrificed at different survival times including 30 minutes (n=2), 2 hours (n=4), 1 to 3 days (n=12), 1 month and 2 months (n=28) after pilocarpine administration.

Immunocytochemistry

Immunocytochemistry for KCC2 was carried out using two polyclonal rabbit KCC2 antisera. The dilution of the first antibody was 1:500 (used only for human tissue) (Williams et al., 1999), whereas it was 1:10 000 for the second antibody (Rivera et al., 1999; Williams et al., 1999). Since the two antibodies showed virtually the same distribution of KCC2, the latter one was used for mouse tissue at a dilution of 1:10 000. For details see *Supplementary experimental procedures.*

Patterns of cell loss

Using a semiquantitative scale, cell loss was classified as Type 1 (mild cell loss), Type 2 (patchy cell loss) or Type 3 in the given region. Type 1: 0-10% of the principal cells were lost, Type 2: 10-50% was missing (referred to as "non-sclerotic"), Type 3: more than 50% of the cells disappeared (referred to as "sclerotic"). In our previous human studies, we found that more than 90% of the CA1 principal cells were missing in the sclerotic type, as described earlier (Karlocai et al., 2011; Magloczky and Freund, 1993; Toth et al., 2010; Wittner et al., 2001).

Western blot analysis

Preparation of crude membrane fractions: Tissue for Western blot analyses was collected from 18 out of 32 epileptic human hippocampi used for immunocytochemistry. The surgically removed tissue was cut into blocks in the coronal plane, and one block containing the hippocampal head was snap-frozen in liquid nitrogen and stored at – 80°C until processing. The adjacent block was processed for immunocytochemistry. Only samples containing all subfields of the hippocampus without considerable portions from other regions were selected for the study. Snap-frozen control hippocampi were kindly provided by the Lenhossek Human Brain Program, Semmelweis University, Budapest (control subjects n=4, males, two of them 37-49 years old, the other two 60-72 years old). For further details see *Supplementary experimental procedures.*

Animal samples were obtained from 10 (6 epileptic, sclerotic, and 4 control) mice. Brains were removed from the skull, cut in half and the right and left hippocampal hemispheres were separated. The right hippocampus was immediately frozen, cut into 2-3 mm thick coronal blocks and regions CA1, CA3 and DG were separated with care. The left hemisphere was processed for

immersion fixation in an identical way to the human tissue, and immunocytochemistry was carried out to verify that cell loss occurred in the animal . For details see *Supplementary experimental procedures.*

Western blotting: Protein samples for SDS-PAGE were prepared in 1x Laemli sample buffer containing 100 mM DTT (final concentration: 2mg/ml), incubated at 65°C for 5-15 min and briefly spun. Afterwards quantities of 10 µl were run on a 10% SDS-PAGE in a Bio-Rad Mini-Protean Dual Slab Cell. The gels were blotted in Towbin's buffer (0.025M Tris, pH 8.3, 0.192M glycine, 20% methanol) for 1 hour at 100V on a 0.2 µm PVDF membrane (Millipore). Immediately after blotting, the membranes were transferred to trays filled with Tris-buffered saline with 0.05% Tween-20 (TBST) (Sigma-Aldrich) and washed 2x5 min at room temperature. Subsequently, the membranes were incubated in 5% non-fat dry milk in TBST at room temperature for 1 hour to block non-specific binding sites and thereafter incubated with rabbit anti-KCC2 (1:10.000, (Williams et al., 1999)), and monoclonal anti-β-actin (1:5000, Sigma) diluted in the same buffer overnight at 4°C. For human samples, the membranes were washed 3x10 min with TBST at room temperature and incubated simultaneously with anti-rabbit alkaline phosphatase conjugate (Sigma, 1:10.000) and anti-mouse alkaline phosphatase (1:7500, Sigma-Aldrich) in 1% BSA-TBST for one hour at room temperature. The membranes were washed 3x10min with TBST at room temperature and developed in NBT- BCIP (nitro-blue tetrazolium and 5-bromo-4-chloro-3'-indolyphosphate). For mouse samples, biotinylated anti-rabbit IgG (1:300, Vector) was applied as secondary serum followed by avidin-biotinylated horseradish peroxidase complex (ABC, 1:300, Vector). Membranes were then incubated in 3,3'-Diaminobenzidine tetrahydrochloride (DAB, Sigma) as a chromogene dissolved in TBST and the immunoperoxidase reaction was developed by 0.01% H_2O_2.

Quantitative analysis: The membranes were scanned on a flat-bed scanner, saved and analysed using Image J, a public domain NIH Image program (developed at the U.S. National Institutes of Health and available on the Internet at http://rsb.info.nih.gov/nih-image/). The optical densities of KCC2-specific bands were measured and normalized to the β-actin values, pooled in three groups for the human tissue (controls, non-sclerotic and sclerotic) and in six groups for the mouse tissue (CA1 sclerotic and control, CA3 sclerotic and control, DG sclerotic and control). Means and standard deviation values were calculated. After a Shapiro normality

test, an independent t- test or Kruskal-Wallis ANOVA followed by a Mann-Whitney U-test were used for statistical analysis with the Statistica 9.1 software.

Dependence of KCC2 immunoreactivity on age, fixation and post-mortem delay

In previous studies we examined several control brains with different post mortem delays and ages of both genders for several antigens (Urban et al., 2002; Wittner et al., 2002). Briefly, the progression of age proved to influence the quality and quantity of immunostaining, i.e., most of the antisera showed weaker staining and lower number of cells in aged subjects. Therefore, subjects older than 80 years have been excluded from the detailed analysis in the present study. For electron microscopic studies (including the present KCC2 experiments) samples were collected with a post-mortem delay of less than 4 hours, since longer post-mortem delays resulted in poor ultrastructural preservation. Electron microscopic analysis of these samples revealed acceptable ultrastructural preservation even in immersion-fixed controls**,** although it was of poorer quality compared to the perfused tissue (HK10 and HK11). The cellular background of immunogold reaction for KCC2 was higher in the control tissue than in the immersion-fixed epileptic samples, except for the post-mortem perfused controls (HK10 and HK11) and HK6. Therefore, these three controls were used for electron microscopic comparison. The preservation of the perfused 2-4 hours post mortem controls (HK10, HK11) and immersion fixed HK6 was comparable to our immersion-fixed epileptic samples and to the perfused animal tissues. KCC2 staining in individual control subjects (and control animals) included in the present study were similar to each other and to previously described immunostaining in the rat (Gulyas et al., 2001).

To examine whether the post-mortem delay *per se* affects the KCC2 immunoreactivity in control samples, eight CD1 mice were anaesthetized with isoflurane, and decapitated after 0, 2 h, 4 h and 6 h, and two individuals were examined at each post mortem time. The brain was removed from the skull, cut into blocks and immersion-fixed in the same way as post mortem human samples (see below). After the same immunocytochemistry protocol, the distribution and intensity of KCC2 immunostaining was compared to perfusion-fixed mouse hippocampi. We found no alteration in KCC2 immunostaining in immersion-fixed mouse hippocampi after 0-4 hour post mortem delay. In mice with 6 hours post mortem delay, a slight increase in intensity

of KCC2 immunoreaction was observed, but the distribution of immunoreactive elements was similar at each time point (Fig. S1).

RESULTS

All patients (n = 32) examined in the present study had pharmacoresistant epilepsy of temporal lobe origin. The seizure focus was identified by multimodal studies including video-EEG monitoring, SPECT and/or PET. Patients with different pathological types (type 1-type 2: non-sclerotic, type 3: sclerotic samples, see Experimental Procedures for details) were included in the study (Table 1). The pattern of hippocampal cell loss was analysed by light microscopy in sections immunostained for different neurochemical markers as shown earlier (Magloczky et al., 2000; Magloczky and Freund, 2005).

We observed fibre reorganization in all groups of patients at the electron microscopic level: mossy fibre reorganization (Magloczky et al., 1997) and sprouting of interneuron axons (Magloczky et al., 2010; Toth et al., 2007; Wittner et al., 2001; Wittner et al., 2002; Wittner et al., 2005) were present in both sclerotic and non-sclerotic TLE patients.

The mouse pilocarpine model of TLE displayed a pattern of cell loss and reorganization very similar to that seen in human tissue (Cavalheiro et al., 1996; Mello et al., 1993). Therefore, we considered them useful for the interpretation of our results concerning alterations of KCC2 expression in TLE patients, and for examination of the time course of changes in KCC2 expression during epileptogenesis. In the acute phase (up to 2 hours after pilocarpine injection) no cell loss was found, either in the strongly epileptic or in the weakly epileptic group animals. In the latent phase (1 day after pilocarpine administration), sensitive cells (certain CA3c pyramidal cells, mossy cells, interneurons) were damaged, but mass cell loss was not observed. At day three, in the strongly epileptic animal group, large numbers of CA1 pyramidal cells showed signs of degeneration. In the chronic phase, a severe cell loss was detected in the CA1-CA3 and hilar regions affecting pyramidal cells and certain types of interneurons (Karlocai et al., 2011; Magloczky et al., 2010), and sclerosis was found in most of the animals in the strong group (over 80% of animals).

Similar to our previous work we found that seizure activity correlated with the cell loss in all three regions (CA1, CA3 and hilus). Correlation proved to be significant by ANOVA in all regions (p<0, 01) (Karlocai et al., 2011).

Light microscopic distribution of KCC2 immunostaining in control and epileptic hippocampi

The expression pattern of KCC2 was studied in the hippocampi of human patients with TLE and in pilocarpine-treated mice. No significant changes were observed between the weakly epileptic and control mice regarding KCC2 expression (not shown) and, therefore, the weakly epileptic animals were not examined further in this study.

Human samples

In control human tissue, KCC2 was found throughout the entire hippocampus, mostly in the dendritic layers. In the somatic region the staining was less intense, only some interneurons showed a rather strong labelling of cell bodies. Interneurons were identified by their laminar distribution and the morphology of their dendrites e.g. smooth dendrites with varicosities, bitufted morphology (see (Freund and Buzsaki, 1996). In the CA1 and CA3 regions of controls, KCC2 was mainly expressed in a subset dendrites (most likely interneuron dendrites, as they were smooth and varicose) (Fig. 1A), and showed a diffuse, faint staining in the entire neuropil with a distribution similar to that described previously in rat (Gulyas et al., 2001). In the *cornu Ammonis*, immunopositive principal cell somata were not observed under our conditions, and the identity of elements of the diffuse neuropil staining could not be clearly recognized at the light microscopic level. The control *hilus* contained a large number of KCC2-positive smooth and spiny dendrites and some faintly stained cell bodies, whereas only a diffuse neuropil staining was observed in the *stratum moleculare* (Fig. 2A, E).

The general intensity of KCC2 expression was considerably increased in the hippocampi of both sclerotic and non-sclerotic TLE patients (Figs. 1 and 2), in parallel with the degree of cell loss (Figs. 1 and 2). A larger amount of discrete, KCC2-immunopositive dendrites could be seen in the CA1 region in all pathological groups, most noticeably in Type 3 (sclerotic) patients (Fig. 1D). Immunopositive dendrites were found throughout the entire width of the remaining

part of the CA1 region. In addition, immunopositive interneuron cell bodies - that are rarely seen in controls - were present in large numbers in the sclerotic hippocampi (Fig. 1D).

In the dentate gyrus, KCC2 expression seemed to be increased as well, and the intensity of the homogeneous staining was enhanced in the molecular layer, especially in Type 3 patients (Fig. 2D). Occasionally, intensely stained complex spines appeared which were never seen in controls (Fig. 2E, F).

We also studied if there was a gender difference in KCC2 upregulation in chronic epilepsy. In case of non-sclerotic samples no such difference was found using the Mann-Whitney U-test ($p=0.67$). In case of sclerotic samples the test could not be carried out due to the very low number of samples deriving from female patients.

Mouse samples

In control mouse tissue, distribution of KCC2 was similar to that observed in human samples as well as in the rat (described by our group earlier (Gulyas et al., 2001)). The protein was abundant throughout the hippocampus with a diffuse neuropil staining in the *cornu Ammonis* and *str. moleculare*. In addition, immunopositive somata and dendrites could be clearly identified in the *hilus* (Fig. 3A).

In epileptic samples with hippocampal sclerosis, the intensity of the staining was considerably increased (similarly to what was found in sclerotic human samples), and this increase was most pronounced in areas with severe cell loss (Fig. 3D). Increased KCC2 staining was mostly found in dendritic regions, e.g. *str. moleculare* (Fig. 3C), and numerous strongly labelled dendrites were observed in CA1, CA3 and *hilus* (Fig. 3C-E). Moreover, a large number of intensely stained KCC2-positive (most probably) mossy and CA3 pyramidal cells were present as well (Fig. 3E, F).

Western blot analysis of KCC2 protein level in control and epileptic hippocampi

Western blot analysis was used to estimate the difference in KCC2 expression levels between control and epileptic tissue. To this end, immune reactions were carried out

simultaneously with highly specific KCC2 and β-actin antibodies (Fig. 4). β-actin was used as an internal control to normalize the KCC2 values. Crude membrane fractions prepared from human tissue obtained from four controls and 18 epileptic patients (n=9, Type 1-2 non-sclerotic, and n=9, Type 3 sclerotic patients) were run on multiple SDS-PAGE gels, blotted and immunostained for KCC2. The normalized KCC2 signal intensity values obtained for control, sclerotic and non-sclerotic hippocampi were averaged and presented as bar-graphs in Fig. 4.

In agreement with our immunohistochemical results, an upregulation of KCC2 was detected with Western blot analysis. The most consistent differences were observed between non-sclerotic epileptic and control patients. In most non-sclerotic epileptic samples studied, KCC2 was significantly upregulated compared to controls, which was reflected in the higher intensity of the 140 kDa band in these patients (Fig. 4A). These results were confirmed by an independent quantitative analysis using densitometry. The non-sclerotic group was found to be significantly different from both the control and the sclerotic group, whereas the sclerotic group did not differ significantly from the control group (pixel density was 138±19 for controls, 212±57 for non-sclerotic and 128 ±19 for sclerotic samples; Kruskal-Wallis ANOVA p=0.006, Mann-Whitney U-test control vs. non-sclerotic p=0.029, sclerotic vs. non-sclerotic p=0.004, and control vs. sclerotic p=0.52, (Fig. 4A, Fig. S2)). Quite large variation was observed in KCC2 immunpositivity among surviving cells in epileptic patients with sclerotic hippocampi. The number of surviving cells in hippocampal subfields varied among individuals, e.g. the number of mossy cells or CA3 pyramidal cells (Lowenstein et al., 1992; Seress et al., 2009).

To examine this possibility further, the hippocampi of control (n=4) and sclerotic mice (n=6) were separated into CA1, CA3 and dentate gyrus (containing the *hilus*) regions, and processed for Western blot analysis. KCC2 and β-actin were visualized with the same antibodies used for human blots. In CA1 and dentate gyrus, a significant increase was found in the intensity of KCC2 expression (pixel density of CA1 control: 149±28 and sclerotic 237±48, pixel density of DG control: 182±20 and sclerotic: 262±22; t-test $p<0.01$ and $p<0.01$ for CA1 and dentate gyrus, respectively). Increase was found in the CA3 region of sclerotic samples as well, although it did not reach the level of significance (pixel density for control: 128±104 and sclerotic: 217±147;t-test p=0.09) (parametric tests were used after Shapiro-normality test).

It is important to note that a large variation was observed among CA3 samples, which may be responsible for the lack of statistical significance (Fig. 4B).

Subcellular localization of KCC2 immunoreactivity in control and epileptic hippocampi

For more detailed investigations, KCC2-immunostained elements were examined at the electron microscopic level in all regions of control and epileptic hippocampi. Visualization of KCC2 was carried out either with DAB or pre-embedding immunogold staining. Both DAB and immunogold labelling was inhomogeneous; staining appeared in clusters in the membrane and never filled it homogeneously. KCC2 appeared in postsynaptic elements, most frequently in dendrites and spines, but rarely in somata. Immunolabelled axons or axon terminals were not seen and, in agreement with lack of KCC2 mRNA in glia (Rivera et al., 1999), glial elements were not stained either, as also reported before (Baldi et al., 2010; Gulyas et al., 2001; Szabadics et al., 2006).

Human samples

In control tissue, mostly dendritic elements and some interneuron somata (see description of interneuron identification) were stained, whereas principal cells very rarely showed KCC2 expression at the level of our detection threshold (Fig. 5C, G).

In epileptic tissue, the overall expression level of KCC2 was increased and new elements became immunoreactive (Fig. 5A, H). However, the majority of the KCC2-immunostained elements remained mostly dendrites and spines that displayed an increased amount of immunopositive clusters (Fig. 5D). A considerable number of KCC2-immunolabelled spines was also present in the epileptic tissue encircled by large mossy terminals in CA3 *strata lucidum* and *pyramidale* (Fig. 5E upper inset). Although KCC2-stained pyramidal cells were not seen in control tissue, KCC2 expression appeared in the somatic membranes of pyramidal cells in all pathological types of epileptic human tissue (Fig. 5A, B). Similarly, granule cell bodies also expressed KCC2 in all types of TLE patients (Fig. 5H), whereas they were mostly immunonegative in control tissue (Fig. 5G). Mossy cell bodies, dendrites and their complex spines were KCC2-immunolabelled both in Type 2 (patchy) and in Type 3 (sclerotic) epileptic human tissue (Fig. 5E, F).

Mouse tissue

The subcellular localization was very similar in mouse and human samples. In control tissue, mostly dendritic shafts (Fig. 6A) and spines receiving asymmetric synapses (Fig. 6G) proved to be immunopositive. Principal cells (Fig. 6C) were mostly free of gold particles, indicating a much lower KCC2 expression, compared to some interneuron somata which were labelled (Fig. 6E).

In the sclerotic mouse tissue (similarly to what we found in human epileptic tissue) the regional distribution of KCC2 was unchanged; however, KCC2 staining appeared to increase in surviving elements throughout the hippocampus. In dendritic elements, the number of gold particles indicating the presence of KCC2 was increased in the CA1 (Fig. 6B), *hilus* (Fig. 6H) and CA3 (Fig. 6I) compared to controls (Fig. 6A, G). Principal cells did not show KCC2 staining in control tissue (Fig. 6C), but the expression of the protein was above detection threshold in the sclerotic mouse tissue (Fig. 6D). In addition, KCC2-stained membrane segments of interneurons became far more abundant in sclerotic tissue compared to controls (Fig. 6F).

DISCUSSION

The main novel finding in the present study is that the overall expression of KCC2 is increased in the hippocampi of TLE patients. This finding is based on the fact that we were able to use well preserved human control tissue for quantitative and qualitative comparisons of KCC2 expression patterns. Parallel experiments were carried out on chronically epileptic mice (and provided essentially identical results) to demonstrate that the upregulation appears in chronic animal models as well. In rodent control tissue KCC2 expression has previously been observed throughout the somadendritic axis of hippocampal principal cells (Baldi et al., 2010), nevertheless, in our samples principal cells showed either very low immunoreactivity or none. This difference is due to the fact that the antibody in our study was used at a more diluted concentration (see *Experimental Procedures*) in order to limit background staining in human samples and to allow detection of a potential upregulation. Indeed, cells containing a

very small amount of KCC2 (e.g. pyramidal cell bodies) appeared virtually negative (likely false-negative) in control tissue, and became immunopositive only in the epileptic tissue when upregulation occurred.

Western blot analysis of KCC2 protein level provided quantitative evidence for the elevation of KCC2 expression in most cases, (except for sclerotic patients where considerable cell loss occurs, thus, concealing protein upregulation). The upregulation is likely explained, at least in part, by the increased KCC2 immunoreactivity of some neurons in epileptic samples. In spite of the well-known loss of certain types of inhibitory cells both in human TLE (de Lanerolle et al., 1988; Magloczky et al., 2000) and animal models of epilepsy (Houser, 1991; Magloczky and Freund, 1993; Martin and Sloviter, 2001), the KCC2-immunopositive interneuron profiles were abundant and contained more numerous immunogold particles in the sclerotic CA1, suggesting that not only the surviving principal cells, but also the surviving interneurons contribute to the enhancement of KCC2 expression.

Increase of the KCC2 transcript (mRNA was quantified with PCR) was found previously in a chronic model of epilepsy (Reid et al., 2001); however, downregulation of KCC2 transcript, protein, and function was observed in slice preparations producing epileptiform activity (Puskarjov et al., 2012; Rivera et al., 2002; Wake et al., 2007) suggesting that acute synchronous firing activity might activate different mechanisms. Nevertheless, the decrease of function may not appear as a global effect; more recent studies have shown that the downregulation is limited to specific areas (Kaila et al., 2014b).

A decrease in KCC2 level occurred in electrically-kindled and pilocarpine-treated mice shortly after the induction of status epilepticus (Barmashenko et al., 2011; Pathak et al., 2007), whereas in the chronic phase KCC2 expression returned to control levels or was even upregulated (Pathak et al., 2007), suggesting that a certain level of reorganization upon seizure activity is necessary for this increase.

In human epileptic peritumoral tissue, elevated levels of NKCC1 and KCC2 were found (Conti et al., 2011), whereas in different types of cortical focal dysplasia, both increased and decreased amounts of KCC2 have been reported (Talos et al., 2012) or an alteration in the subcellular distribution of KCC2 has been observed (Aronica et al., 2007).

The large variability of the findings regarding KCC2 levels in epileptic tissue is likely due to differences in epilepsy models (Barmashenko et al., 2011; Rivera et al., 2002), phases

(acute, latent, chronic (Pathak et al., 2007) and the regions studied e.g. neocortex (Aronica et al., 2007; Bragin et al., 2009; Talos et al., 2012), hippocampus (Munoz et al., 2007), or subiculum (Huberfeld et al., 2007; Munoz et al., 2007). Notably, however, the above studies do not shed light on differences in KCC2 expression that exist between the healthy and chronically epileptic human hippocampus.

The present study highlights the finding that the upregulation of KCC2 can vary among hippocampal regions. Thus, in experiments examining changes of KCC2 content in the entire hippocampus (Li et al., 2008) some areas with massive cell- as well as KCC2 loss may have masked the upregulation occurring in specific regions. Thus, the degree and pattern of cell loss may differ among individuals, resulting in a variability regarding the extent of KCC2 upregulation.

Epileptic seizures are known to cause massive interneuron activity leading to a high Cl^- load. Consequently, KCC2 would keep functioning in an extrusion mode, contributing to a pro-excitatory elevation in extracellular K^+ (Kaila et al., 1997; Kaila et al., 2014b; Smirnov et al., 1999; Viitanen et al., 2010). Moreover, gold particles indicating the presence of KCC2 protein are most often found near asymmetric (excitatory) synapses and very rarely near symmetric synapses (Gulyas et al., 2001) indicating that a major role of KCC2 upregulation might well be linked to changes in excitability at the single synapse level.

The importance of KCC2 function near excitatory synapses is supported by results demonstrating its role in dendritic spinogenesis. Both *in vitro* (Li et al., 2007) and *in vivo* (Gauvain et al., 2011) studies have shown that KCC2 promotes spine development by interacting with the cytoskeleton, and its presence is necessary for the aggregation of postsynaptic GluR1 containing AMPA receptors (Fiumelli et al., 2013; Gauvain et al., 2011).

Previous studies have shown that a generalized spine loss occurs immediately after acute status epilepticus. However, this damage was transient and was followed by recovery in the chronic phase (Isokawa, 2000). Since changes in KCC2 expression paralleled these changes (decrease in the acute phase, recovery and increase in the chronic phase), the upregulation of KCC2 seems to play an essential role in the recovery of spine density and the aggregation of certain AMPA subunits (Fiumelli et al., 2013; Gauvain et al., 2011). These

findings are in line with a recent study showing that an abnormal human variant of the KCC2 protein disrupts both Cl^- extrusion and dendritic spinogenesis (Puskarjov et al., 2014).

Consequences of KCC2 upregulation

At the network level the increase of KCC2 would appear as proepileptic, since it increases excitability by supporting the rearrangement of dendritic spines and the aggregation of AMPA receptors. Moreover, it would further increase excitability by enhancing GABAergic $[K^+]_o$ transients leading to the depolarization of neighbouring cells (Kaila et al., 1997; Viitanen et al., 2010). However, at the cellular level, the upregulation could act in a neuroprotective manner, since the sustained extrusion mode of KCC2 would effectively export Cl^- which is a prerequisite for efficient inhibition regardless of whether it is hyperpolarizing or "shunting" (for discussion, see (Kaila et al., 2014a). At the subcellular level, the effect of a KCC2 increase will depend on its localization. In dendritic spines KCC2 function might be mainly linked to the rearrangement of spines and aggregation of GluR1-containing AMPA receptors (Fiumelli et al., 2013; Gauvain et al., 2011), thus, altering the excitability of the cell. On dendritic shafts the increased KCC2 amount would play a role in changes of the cytoskeleton and provide a GABAergic $[K^+]_o$ transient (Viitanen et al., 2010). Similarly, in the perisomatic region, inhibition will increase intracellular $[Cl^-]$, triggering the extrusion of Cl^- and K^+ via KCC2. As a result, release of K^+ mediated by phasic inhibition will contribute to the pacing of the synchronous discharges during epileptic activity. Notably, there is an accumulating amount of evidence supporting the idea that interneurons are involved also in the triggering of seizures (de Curtis and Gnatkovsky, 2009; Gnatkovsky et al., 2008).

The above discussion reflects the well-known fact that the influence of disease-related changes in signalling mechanisms at the molecular and cellular level have context-dependent effects (Kaila et al., 2014b). Moreover, alterations in ionic regulation that alter neuronal signalling ("ionic plasticity") are likely to have several kinds of both disease-promoting as well as adaptive actions in epileptogenesis and in seizure generation as reviewed recently (Kaila et al., 2014b). Thus, it remains to be established whether the elevation of KCC2 expression is ultimately a pro- or anticonvulsive change, perhaps exerting

qualitatively distinct actions during e.g. ictal and interictal states or during the course of disease progression.

Since cation-chloride cotransporters are potential targets of antiepileptic drug development (Kahle et al., 2013; Loscher et al., 2013), it is essential to clarify their changes in the brains of human TLE patients. This task is made easier by the recent description of the spatiotemporal expression profiles of the entire CCC family in the human brain along with important functionally associated molecules (Sedmak et al, 2015, in press). According to the present results and earlier data in chronic TLE (Galanopoulou, 2008; Pathak et al., 2007), KCC2 expression appears elevated in the epileptic hippocampus. Further studies using, for instance, phosphoantibodies (Kahle et al., 2013) are needed to gain more insight into the functional relevance of KCC2 upregulation in various neuronal populations.

Acknowledgements

The authors are grateful to Drs. M. Palkovits, P. Sótonyi and Zs. Borostyánkői (Semmelweis University, Budapest) for providing control human tissue. We thank Mr. Gergő Botond for his helpful suggestions regarding Western blot experiments. The excellent technical assistance of Ms. E. Simon, K. Lengyel, Mr. Gy. Goda is also acknowledged. This study was supported by grants from OTKA 102802 Hungary, and NS030549NIH.

Figure Legends

Figure 1: Light micrographs showing the distribution of KCC2-positive elements in the human CA1 *stratum oriens* of control (A) and different types of epileptic hippocampi (B, C and D). Discrete, intense dendritic staining of individual interneurons (arrowheads, A, B, C and D) is embedded in a weaker, diffuse neuropil staining. The number of KCC2-immunostained dendrites is increased in the epileptic CA1 region, in parallel with the degree of principal cell loss (B, C, and D). The highest density of immunostained profiles is seen in the sclerotic CA1

(D), where KCC2-immunoreactive interneuron somata are also frequently observed (arrows in D). Scales: A-D: 50 µm
CA1: Cornu Ammonis region 1, KCC2: Potassium-chloride cotransporter-2

Figure 2: Light micrographs showing the distribution of KCC2-positive elements in the dentate gyrus of human control (A and E) and epileptic samples with different pathology (B, C, D and F). In controls, discrete interneuron dendrites are visible in the *stratum moleculare* and in the hilus (A, arrows). The number of immunopositive dendrites is increased in epileptic samples (B, C and D, arrows) and the intensity of faint diffuse staining of the *stratum moleculare* is enhanced. In addition, the density of KCC2-immunostained elements – smooth and spiny dendrites (arrows in E) - is profoundly enhanced in the *hilus* of Type 2 and 3 patients (C, D and F). Spines, dendrites and cell bodies of surviving mossy cells (F, large arrows), and dendrites with long, complex spines (F, small arrows), show intense KCC2-immunopositivity. Scales: A-D: 150µm; E, F: 50 µm
DG: Dentate Gyrus, KCC2: Potassium-chloride cotransporter-2

Figure 3: Light micrographs showing the distribution of KCC2-positive elements in the dentate gyrus and CA1 regions of control (A and B) and epileptic (sclerotic) mice (C and D). In control, discrete dendrites are visible in the *hilus* (arrows), whereas diffuse staining of the neuropil occurs in *stratum moleculare* of DG (A) and in *strata oriens* and *radiatum* of CA1 (B). In epileptic samples, the number of immunopositive dendrites is increased (arrows on C, D and E) and the intensity of faint diffuse staining of the *stratum moleculare* is enhanced (C). In addition, the occurrence of KCC2-immunostained somata is increased, both in the *hilus* (arrows on C and F) and in the *cornu Ammonis* (D and E). Scales: A-D: 50µm
CA1: cornu Ammonis region 1, DG: Dentate Gyrus, KCC2: Potassium-chloride cotransporter-2

Figure 4. Western blot of crude membrane fractions isolated from epileptic and control hippocampi show an upregulation of KCC2. In human tissue, 4 controls were compared to 9 non-sclerotic and 9 sclerotic samples (patients). Significant differences were found among control and non-sclerotic samples; however patients with sclerotic hippocampi showed no significant difference compared to control (though 5 out of 9 patients displayed elevated KCC2

levels compared to the controls) (A). In the epileptic sclerotic mouse hippocampus, CA1 CA3 and DG were separated and compared to controls. A significant increase of KCC2 was found in sclerotic CA1 and DG but not in CA3 (B).
CA1: Cornu Ammonis region 1, CA3: Cornu Ammonis region 3, DG: Dentate Gyrus, KCC2: Potassium-chloride cotransporter-2, TLE: Temporal Lobe Epilepsy

Figure 5: Electron micrographs show preembedding immunogold and DAB labelling of KCC2 in human tissue. Silver-enhanced gold particles signalling KCC2-immunopositivity are present on the membrane of CA1 pyramidal cell bodies of TLE patients (A and B, arrows); the same cell is shown at the light microscopic level in the upper right small insert in A. The framed area is shown at higher power in B. Spines of principal cells receiving asymmetric synaptic input were also intensively KCC2-immunoreactive (C, arrows), similarly to interneuron dendrites receiving multiple asymmetric synaptic contacts (asterisks) are shown in D. Mossy cell bodies (lower insert in E shows the same cell at the light microscopic level) and their dendrites and spines (see small upper insert, sp: spine, mt: mossy terminal) are also positive for KCC2 in epileptic samples. The framed area is shown at higher power in F, arrows point to the silver-enhanced gold particles. Granule cell bodies are negative for KCC2 in the control (G), whereas their dendrites and somata contain numerous silver-enhanced gold particles in the epileptic cases (H, small arrows). Asterisks indicate synapses. Scales: A, E: 5 µm; B, F: 2 µm; G, H: 2.5µm; C, D: 0.5µm
CA1: Cornu Ammonis region1, DG: Dentate Gyrus, KCC2: Potassium-chloride cotransporter-2, TLE: Temporal Lobe Epilepsy

Figure 6: Electron micrographs show preembedding immunogold labelling of KCC2 in the mouse hippocampus. In control tissue silver-enhanced gold particles indicating KCC2-immunopositivity are present in the membrane of dendrites (A, arrows), and in dendritic spines (G). Principal cell somata appear free of staining (C) whereas the cell body of interneurons may express KCC2 (see arrow in E). In epileptic tissue, the density of sliver-enhanced gold particles is increased in dendrites and dendritic spines (B, H, I). Principal cell somata become positive for KCC2 (D), and a strong upregulation of KCC2-expression can be seen in the membrane of certain interneurons (F). Silver-enhanced gold particles are usually present extrasynaptically,

near asymmetric synapses (B, H and I). Asterisks indicate synapses. Scales: A, B and G-I: 0,2 µm; C-F: 0,5µm

CA1: Cornu Ammonis region1, CA3: Cornu Ammonis region 3, DG: Dentate Gyrus, KCC2: Potassium-chloride cotransporter-2

References

Aronica, E., et al., 2007. Differential expression patterns of chloride transporters, Na+-K+-2Cl--cotransporter and K+-Cl--cotransporter, in epilepsy-associated malformations of cortical development. Neuroscience. 145**,** 185-96.

Babb, T.L., et al., 1989. Glutamate decarboxylase-immunoreactive neurons are preserved in human epileptic hippocampus. J Neurosci. 9**,** 2562-74.

Baldi, R., Varga, C., Tamas, G., 2010. Differential distribution of KCC2 along the axo-somato-dendritic axis of hippocampal principal cells. Eur J Neurosci. 32**,** 1319-25.

Barmashenko, G., et al., 2011. Positive shifts of the GABAA receptor reversal potential due to altered chloride homeostasis is widespread after status epilepticus. Epilepsia. 52**,** 1570-8.

Blackwood, W., Corsellis, J.A.N., 1976. Greenfield's Neuropathology, Vol., Edward Arnold, London.

Bragin, D.E., et al., 2009. Development of epileptiform excitability in the deep entorhinal cortex after status epilepticus. Eur J Neurosci. 30**,** 611-24.

Buckmaster, P.S., Dudek, F.E., 1997. Neuron loss, granule cell axon reorganization, and functional changes in the dentate gyrus of epileptic kainate-treated rats. J Comp Neurol. 385**,** 385-404.

Cavalheiro, E.A., Santos, N.F., Priel, M.R., 1996. The pilocarpine model of epilepsy in mice. Epilepsia. 37**,** 1015-9.

Cohen, I., et al., 2002. On the origin of interictal activity in human temporal lobe epilepsy in vitro. Science. 298**,** 1418-21.

Colder, B.W., et al., 1996. Decreased neuronal burst discharge near site of seizure onset in epileptic human temporal lobes. Epilepsia. 37**,** 113-21.

Conti, L., et al., 2011. Anomalous levels of Cl- transporters cause a decrease of GABAergic inhibition in human peritumoral epileptic cortex. Epilepsia. 52**,** 1635-44.

Corsellis, J.A.N., 1955. The incidence of Ammon's horn sclerosis. Brain. 80**,** 193-208.

Cossart, R., et al., 2001. Dendritic but not somatic GABAergic inhibition is decreased in experimental epilepsy. Nat Neurosci. 4**,** 52-62.

de Curtis, M., Gnatkovsky, V., 2009. Reevaluating the mechanisms of focal ictogenesis: The role of low-voltage fast activity. Epilepsia. 50**,** 2514-25.

de Lanerolle, N.C., et al., 1988. Evidence for hippocampal interneuron loss in human temporal lobe epilepsy. Epilepsia. 29**,** 674.
de Lanerolle, N.C., et al., 1989. Hippocampal interneuron loss and plasticity in human temporal lobe epilepsy. Brain Res. 495**,** 387-95.
de Lanerolle, N.C., et al., 2003. A retrospective analysis of hippocampal pathology in human temporal lobe epilepsy: evidence for distinctive patient subcategories. Epilepsia. 44**,** 677-87.
Fiumelli, H., et al., 2013. An ion transport-independent role for the cation-chloride cotransporter KCC2 in dendritic spinogenesis in vivo. Cereb Cortex. 23**,** 378-88.
Freund, T.F., Buzsaki, G., 1996. Interneurons of the hippocampus. Hippocampus. 6**,** 347-470.
Fujiwara-Tsukamoto, Y., et al., 2003. Excitatory GABA input directly drives seizure-like rhythmic synchronization in mature hippocampal CA1 pyramidal cells. Neuroscience. 119**,** 265-75.
Galanopoulou, A.S., 2008. Dissociated gender-specific effects of recurrent seizures on GABA signaling in CA1 pyramidal neurons: role of GABA(A) receptors. J Neurosci. 28**,** 1557-67.
Gauvain, G., et al., 2011. The neuronal K-Cl cotransporter KCC2 influences postsynaptic AMPA receptor content and lateral diffusion in dendritic spines. Proc Natl Acad Sci U S A. 108**,** 15474-9.
Gnatkovsky, V., et al., 2008. Fast activity at seizure onset is mediated by inhibitory circuits in the entorhinal cortex in vitro. Ann Neurol. 64**,** 674-86.
Green, R.C., 1991. Neuropathology and behavior in epilepsy. In: Epilepsy and Behavior. Vol., ed.^eds. Wiley-Liss, Inc., pp. 345-359.
Gulyas, A.I., et al., 2001. The KCl cotransporter, KCC2, is highly expressed in the vicinity of excitatory synapses in the rat hippocampus. Eur J Neurosci. 13**,** 2205-17.
Heinemann, U., et al., 2000. Alterations of glial cell function in temporal lobe epilepsy. Epilepsia. 41**,** S185-9.
Hoffmann, E.K., Dunham, P.B., 1995. Membrane mechanisms and intracellular signalling in cell volume regulation. Int Rev Cytol. 161**,** 173-262.
Houser, C.R., 1991. GABA neurons in seizure disorders: a review of immunocytochemical studies. Neurochem Res. 16**,** 295-308.
Huberfeld, G., et al., 2007. Perturbed chloride homeostasis and GABAergic signaling in human temporal lobe epilepsy. J Neurosci. 27**,** 9866-73.
Isokawa, M., 2000. Remodeling dendritic spines of dentate granule cells in temporal lobe epilepsy patients and the rat pilocarpine model. Epilepsia. 41 Suppl 6**,** S14-7.
Jaenisch, N., Witte, O.W., Frahm, C., 2010. Downregulation of potassium chloride cotransporter KCC2 after transient focal cerebral ischemia. Stroke. 41**,** e151-9.
Kahle, K.T., et al., 2013. Modulation of neuronal activity by phosphorylation of the K-Cl cotransporter KCC2. Trends Neurosci. 36**,** 726-37.
Kaila, K., et al., 1997. Long-lasting GABA-mediated depolarization evoked by high-frequency stimulation in pyramidal neurons of rat hippocampal slice is attributable to a network-driven, bicarbonate-dependent K+ transient. J Neurosci. 17**,** 7662-72.
Kaila, K., et al., 2014a. Cation-chloride cotransporters in neuronal development, plasticity and disease. Nat Rev Neurosci. 15**,** 637-54.
Kaila, K., et al., 2014b. GABA actions and ionic plasticity in epilepsy. Curr Opin Neurobiol. 26**,** 34-41.

Karlocai, M.R., et al., 2011. Redistribution of CB1 Cannabinoid Receptors in the Acute and Chronic Phases of Pilocarpine-Induced Epilepsy. PloS one. 6**,** e27196.
Lang, F., et al., 1998. Functional significance of cell volume regulatory mechanisms. Physiol Rev. 78**,** 247-306.
Laurberg, S., Zimmer, J., 1981. Lesion-induced sprouting of hippocampal mossy fiber collaterals to the fascia dentata in developing and adult rats. J Comp Neurol. 200**,** 433-59.
Li, H., et al., 2007. KCC2 interacts with the dendritic cytoskeleton to promote spine development. Neuron. 56**,** 1019-33.
Li, X., et al., 2008. Long-term expressional changes of Na+ -K+ -Cl- co-transporter 1 (NKCC1) and K+ -Cl- co-transporter 2 (KCC2) in CA1 region of hippocampus following lithium-pilocarpine induced status epilepticus (PISE). Brain research. 1221**,** 141-6.
Loscher, W., Puskarjov, M., Kaila, K., 2013. Cation-chloride cotransporters NKCC1 and KCC2 as potential targets for novel antiepileptic and antiepileptogenic treatments. Neuropharmacology. 69**,** 62-74.
Lowenstein, D.H., et al., 1992. Selective vulnerability of dentate hilar neurons following traumatic brain injury: a potential mechanistic link between head trauma and disorders of the hippocampus. J Neurosci. 12**,** 4846-53.
Magloczky, Z., Freund, T.F., 1993. Selective neuronal death in the contralateral hippocampus following unilateral kainate injections into the CA3 subfield. Neuroscience. 56**,** 317-35.
Magloczky, Z., et al., 1997. Loss of Calbindin-D28K immunoreactivity from dentate granule cells in human temporal lobe epilepsy. Neuroscience. 76**,** 377-85.
Magloczky, Z., et al., 2000. Changes in the distribution and connectivity of interneurons in the epileptic human dentate gyrus. Neuroscience. 96**,** 7-25.
Magloczky, Z., Freund, T.F., 2005. Impaired and repaired inhibitory circuits in the epileptic human hippocampus. Trends Neurosci. 28**,** 334-40.
Magloczky, Z., 2010. Sprouting in human temporal lobe epilepsy: excitatory pathways and axons of interneurons. Epilepsy Res. 89**,** 52-9.
Magloczky, Z., et al., 2010. Dynamic changes of CB1-receptor expression in hippocampi of epileptic mice and humans. Epilepsia. 51 Suppl 3**,** 115-20.
Margerison, J.H., Corsellis, J.A.N., 1966. Epilepsy and the temporal lobe. Brain. 89**,** 499-530.
Martin, J.L., Sloviter, R.S., 2001. Focal inhibitory interneuron loss and principal cell hyperexcitability in the rat hippocampus after microinjection of a neurotoxic conjugate of saporin and a peptidase-resistant analog of Substance P. J Comp Neurol. 436**,** 127-52.
Mathern, G.W., Babb, T.L., Armstrong, D.L., 1997a. Hippocampal Sclerosis. In: Epilepsy: A Comprehensive Textbook. Vol. 13, J.J. Engel, T.A. Pedley, ed.^eds. Lipincott-Raven, Philadelphia, pp. 133-155.
Mathern, G.W., et al., 1997b. Human hippocampal AMPA and NMDA mRNA levels in temporal lobe epilepsy patients. Brain. 120**,** 1937-59.
Mathern, G.W., et al., 1998. Altered hippocampal kainate-receptor mRNA levels in temporal lobe epilepsy patients. Neurobiol Dis. 5**,** 151-76.
McNamara, J.O., 1999. Emerging insights into the genesis of epilepsy. Nature. 399**,** A15-22.
Mello, L.E., et al., 1993. Circuit mechanisms of seizures in the pilocarpine model of chronic epilepsy: cell loss and mossy fiber sprouting. Epilepsia. 34**,** 985-95.
Mody, I., et al., 1995. GABAergic inhibition of granule cells and hilar neuronal synchrony following ischemia-induced hilar neuronal loss. Neuroscience. 69**,** 139-50.

Munoz, A., et al., 2007. Cation-chloride cotransporters and GABA-ergic innervation in the human epileptic hippocampus. Epilepsia. 48**,** 663-73.
Okabe, A., et al., 2003. Changes in chloride homeostasis-regulating gene expressions in the rat hippocampus following amygdala kindling. Brain Res. 990**,** 221-6.
Papp, E., et al., 2008. Relationship between neuronal vulnerability and potassium-chloride cotransporter 2 immunoreactivity in hippocampus following transient forebrain ischemia. Neuroscience. 154**,** 677-89.
Pathak, H.R., et al., 2007. Disrupted dentate granule cell chloride regulation enhances synaptic excitability during development of temporal lobe epilepsy. The Journal of neuroscience : the official journal of the Society for Neuroscience. 27**,** 14012-22.
Payne, J.A., Stevenson, T.J., Donaldson, L.F., 1996. Molecular characterization of a putative K-Cl cotransporter in rat brain. A neuronal-specific isoform. J Biol Chem. 271**,** 16245-52.
Payne, J.A., 1997. Functional characterization of the neuronal-specific K-Cl cotransporter: implications for [K+]o regulation. Am J Physiol. 273**,** C1516-25.
Puskarjov, M., et al., 2012. Activity-dependent cleavage of the K-Cl cotransporter KCC2 mediated by calcium-activated protease calpain. J Neurosci. 32**,** 11356-64.
Puskarjov, M., et al., 2014. A variant of KCC2 from patients with febrile seizures impairs neuronal Cl- extrusion and dendritic spine formation. EMBO Rep. 15**,** 723-9.
Reid, K.H., et al., 2001. The mRNA level of the potassium-chloride cotransporter KCC2 covaries with seizure susceptibility in inferior colliculus of the post-ischemic audiogenic seizure-prone rat. Neurosci Lett. 308**,** 29-32.
Rivera, C., et al., 1999. The K+/Cl- co-transporter KCC2 renders GABA hyperpolarizing during neuronal maturation. Nature. 397**,** 251-5.
Rivera, C., et al., 2002. BDNF-induced TrkB activation down-regulates the K+-Cl- cotransporter KCC2 and impairs neuronal Cl- extrusion. J Cell Biol. 159**,** 747-52.
Robbins, R.J., et al., 1991. A selective loss of somatostatin in the hippocampus of patients with temporal lobe epilepsy. Ann Neurol. 29**,** 325-32.
Seress, L., et al., 2009. Survival of mossy cells of the hippocampal dentate gyrus in humans with mesial temporal lobe epilepsy Clinical article. Journal of Neurosurgery. 111**,** 1237-1247.
Sloviter, R.S., 1987. Decreased hippocampal inhibition and a selective loss of interneurons in experimental epilepsy. Science. 235**,** 73-6.
Smirnov, S., et al., 1999. Pharmacological isolation of the synaptic and nonsynaptic components of the GABA-mediated biphasic response in rat CA1 hippocampal pyramidal cells. J Neurosci. 19**,** 9252-60.
Spencer, D.D., Spencer, S.S., 1985. Surgery for epilepsy. Neurol Clin. 3**,** 313-30.
Stein, V., Nicoll, R.A., 2003. GABA generates excitement. Neuron. 37**,** 375-8.
Stewart, T.H., et al., 2010. Chronic dysfunction of astrocytic inwardly rectifying K+ channels specific to the neocortical epileptic focus after fluid percussion injury in the rat. J Neurophysiol. 104**,** 3345-60.
Sutula, T., et al., 1989. Mossy fiber synaptic reorganization in the epileptic human temporal lobe. Ann Neurol. 26**,** 321-30.
Swann, J.W., et al., 2000. Spine loss and other dendritic abnormalities in epilepsy. Hippocampus. 10**,** 617-25.
Szabadics, J., et al., 2006. Excitatory effect of GABAergic axo-axonic cells in cortical microcircuits. Science. 311**,** 233-5.

Talos, D.M., et al., 2012. Altered inhibition in tuberous sclerosis and type IIb cortical dysplasia. Ann Neurol. 71**,** 539-51.
Toth, K., et al., 2007. Morphology and synaptic input of substance P receptor-immunoreactive interneurons in control and epileptic human hippocampus. Neuroscience. 144**,** 495-508.
Toth, K., et al., 2010. Loss and reorganization of calretinin-containing interneurons in the epileptic human hippocampus. Brain. 133**,** 2763-77.
Urban, Z., Magloczky, Z., Freund, T.F., 2002. Calretinin-containing interneurons innervate both principal cells and interneurons in the CA1 region of the human hippocampus. Acta Biol Hung. 53**,** 205-20.
Viitanen, T., et al., 2010. The K+-Cl cotransporter KCC2 promotes GABAergic excitation in the mature rat hippocampus. J Physiol. 588**,** 1527-40.
Wake, H., et al., 2007. Early changes in KCC2 phosphorylation in response to neuronal stress result in functional downregulation. The Journal of neuroscience. 27**,** 1642-50.
Williams, J.R., et al., 1999. The neuron-specific K-Cl cotransporter, KCC2. Antibody development and initial characterization of the protein. J Biol Chem. 274**,** 12656-64.
Wilson, C.L., et al., 1998. Paired pulse suppression and facilitation in human epileptogenic hippocampal formation. Epilepsy Res. 31**,** 211-30.
Wilson, C.L., 1999. Neurophysiology of epileptic limbic pathways in intact human temporal lobe. In: The Epilepsies. Etiologies and prevention. Vol., P.K.a.H.O. Lüders, ed.^eds. Academic Press, San Diego, USA, pp. 171-179.
Wittner, L., et al., 2001. Preservation of perisomatic inhibitory input of granule cells in the epileptic human dentate gyrus. Neuroscience. 108**,** 587-600.
Wittner, L., et al., 2002. Synaptic reorganization of calbindin-positive neurons in the human hippocampal CA1 region in temporal lobe epilepsy. Neuroscience. 115**,** 961-78.
Wittner, L., et al., 2005. Surviving CA1 pyramidal cells receive intact perisomatic inhibitory input in the human epileptic hippocampus. Brain. 128**,** 138-52.
Ylinen, A., et al., 1991. Behavioural, electrophysiological and histopathological changes following sustained stimulation of the perforant pathway input to the hippocampus: effect of the NMDA receptor antagonist, CGP 39551. Brain Res. 553**,** 195-200.
Zhang, W., et al., 2009. Surviving hilar somatostatin interneurons enlarge, sprout axons, and form new synapses with granule cells in a mouse model of temporal lobe epilepsy. J Neurosci. 29**,** 14247-56.
Zhu, Z.Q., et al., 1997. Disproportionate loss of CA4 parvalbumin-immunoreactive interneurons in patients with Ammon's horn sclerosis. J Neuropathol Exp Neurol. 56**,** 988-98.
G. Sedmak, N. Jovanov-Miloševic, M. Puskarjov, M. Ulamec, B. Krušlin, Kai Kaila, Milos Judas (2015). Developmental expression patterns of KCC2 and functionally associated molecules in the human brain (Cerebral Cortex, in press).

Figure Legends

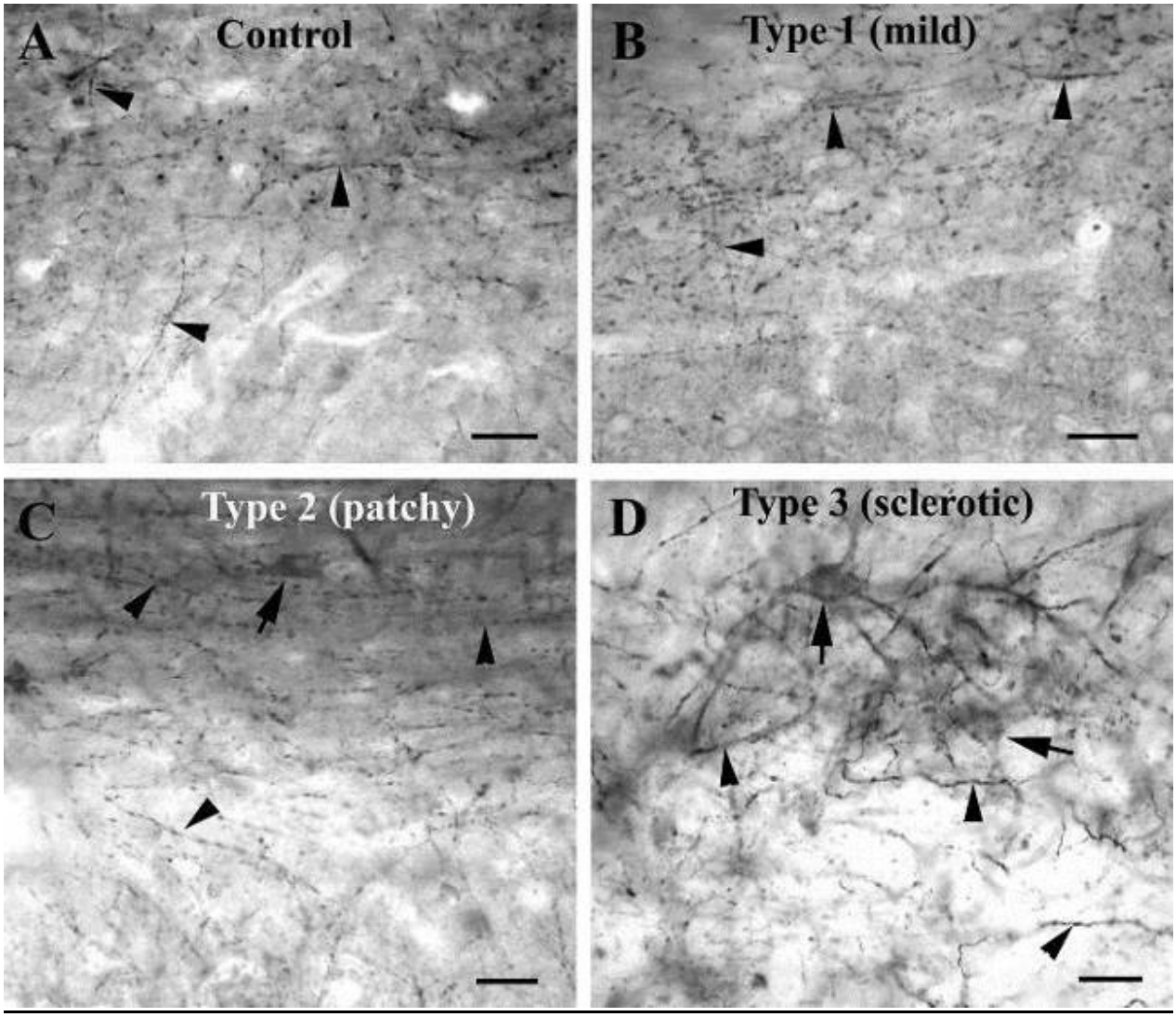

Figure 1: Light micrographs showing the distribution of KCC2-positive elements in the human CA1 *stratum oriens* of control (A) and different types of epileptic hippocampi (B, C and D). Discrete, intense dendritic staining of individual interneurons (arrowheads, A, B, C and D) is embedded in a weaker, diffuse neuropil staining. The number of KCC2-immunostained dendrites is increased in the epileptic CA1 region, in parallel with the degree of principal cell loss (B, C, and D). The highest density of immunostained profiles is seen in the sclerotic CA1 (D), where KCC2-immunoreactive interneuron somata are also frequently observed (arrows in D). Scales: A-D: 50 µm

CA1: Cornu Ammonis region 1, KCC2: Type 2 potassium-chloride cotransporter

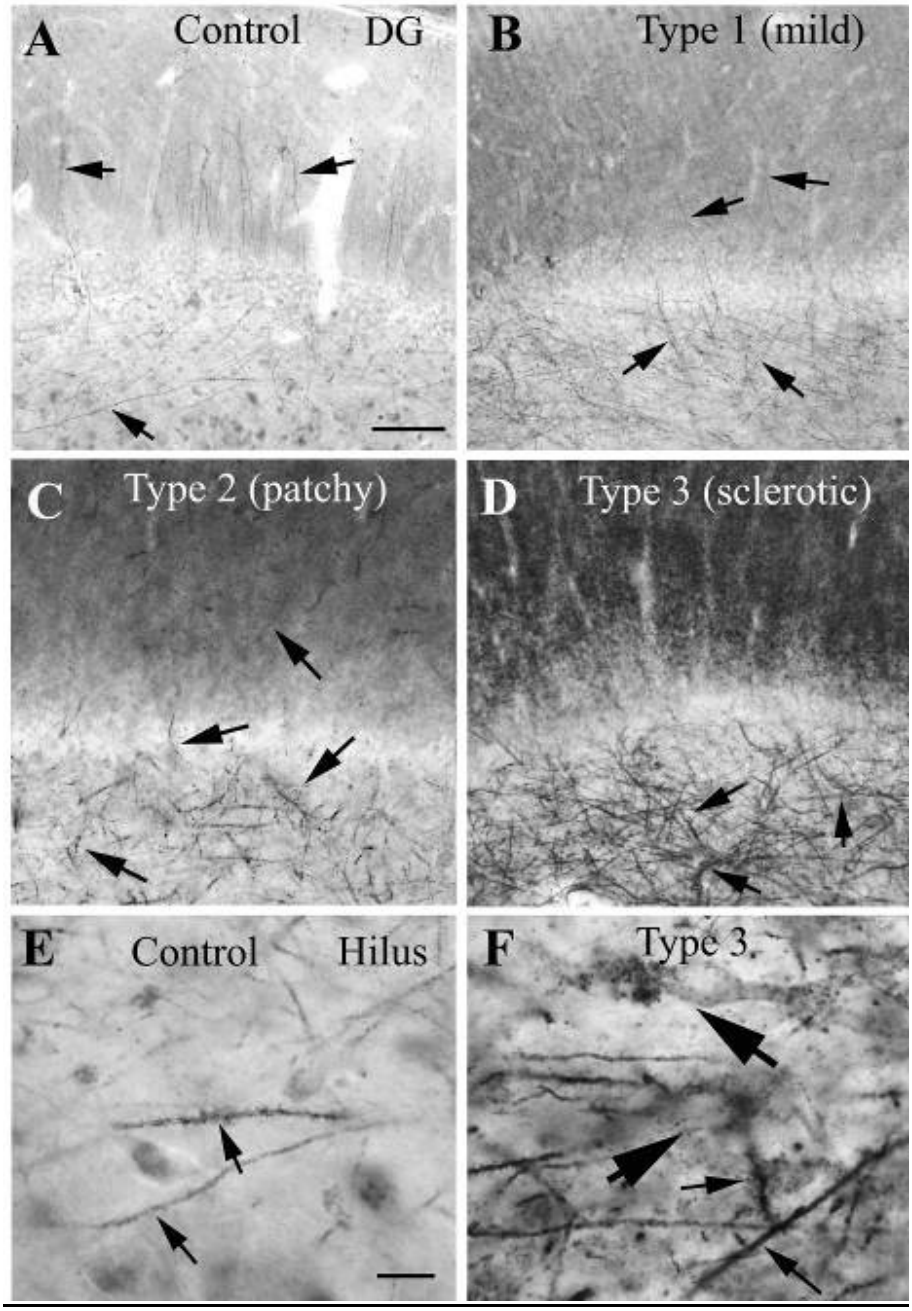

Figure 2: Light micrographs showing the distribution of KCC2-positive elements in the dentate gyrus of human control (A and E) and epileptic samples with different pathology (B, C, D and F). In controls, discrete interneuron dendrites are visible in the *stratum moleculare* and in the hilus (A, arrows). The number of immunopositive dendrites is increased in epileptic samples (B, C and D, arrows) and the intensity of faint diffuse staining of the *stratum moleculare* is enhanced. In addition, the density of KCC2-immunostained elements – smooth and spiny

dendrites (arrows in E) - is profoundly enhanced in the *hilus* of Type 2 and 3 patients (C, D and F). Spines, dendrites and cell bodies of surviving mossy cells (F, large arrows), and dendrites with long, complex spines (F, small arrows), show intense KCC2-immunopositivity. Scales: A-D: 150µm; E, F: 50 µm

DG: Dentate Gyrus, KCC2: Type 2 potassium-chloride cotransporter

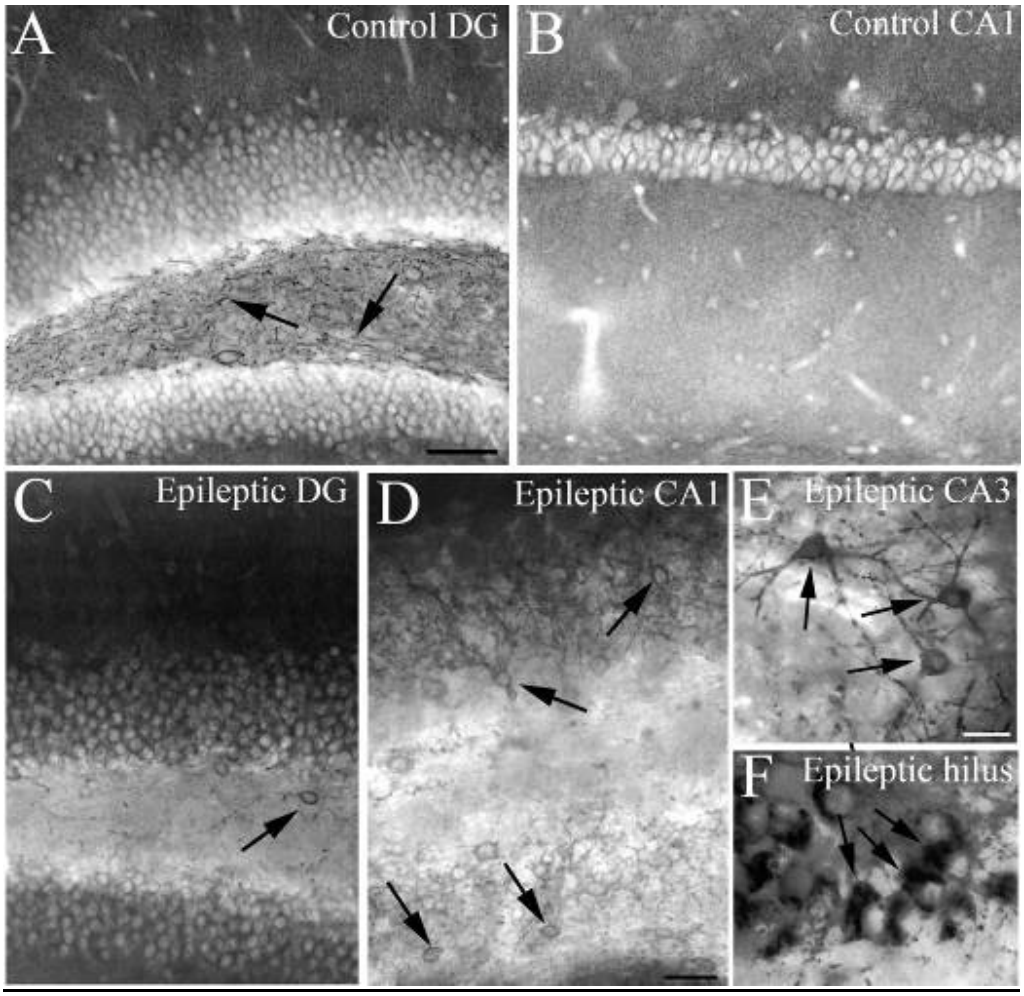

Figure 3: Light micrographs showing the distribution of KCC2-positive elements in the dentate gyrus and CA1 regions of control (A and B) and epileptic (sclerotic) mice (C and D). In control, discrete dendrites are visible in the *hilus* (arrows), whereas diffuse staining of the neuropil occurs in *stratum moleculare* of DG (A) and in *strata oriens* and *radiatum* of CA1 (B). In epileptic samples, the number of immunopositive dendrites is increased (arrows on C, D and E) and the intensity of faint diffuse staining of the *stratum moleculare* is enhanced (C). In addition,

the occurrence of KCC2-immunostained somata is increased, both in the *hilus* (arrows on C and F) and in the *cornu Ammonis* (D and E). Scales: A-D: 50µm

DG: Dentate Gyrus, KCC2: Type 2 potassium-chloride cotransporter

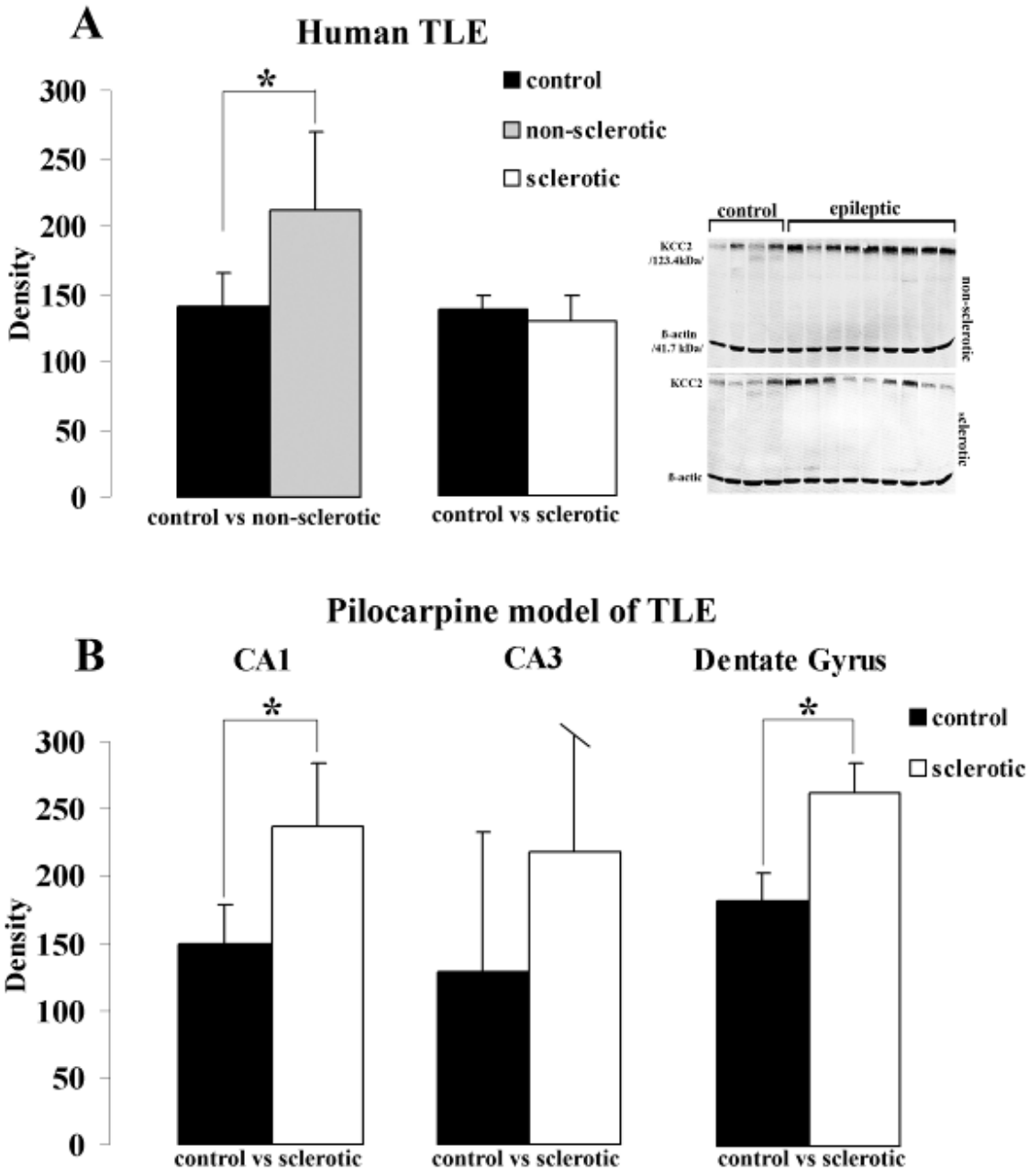

Figure 4. Western blot of membrane fractions isolated from epileptic and control hippocampi show an upregulation of KCC2. In human tissue, 4 controls were compared to 9 non-sclerotic and 9 sclerotic samples, however, due to differences in post-mortem times, only three controls were included in statistics (fourth band was excluded). Significant differences were found among control and non-sclerotic samples; however patients with sclerotic hippocampi showed no significant difference compared to control (though 5 out of 9 patients displayed elevated KCC2 levels compared to the controls) (A). In the epileptic sclerotic mouse hippocampus, CA1 CA3 and DG were separated and compared to controls. A significant increase of KCC2 was found in sclerotic CA1 and DG but not in CA3 (B).

CA1: Cornu Ammonis region1, CA3: Cornu Ammonis region 3, DG: Dentate Gyrus, KCC2: Type 2 potassium-chloride cotransporter, TLE: Temporal Lobe Epilepsy

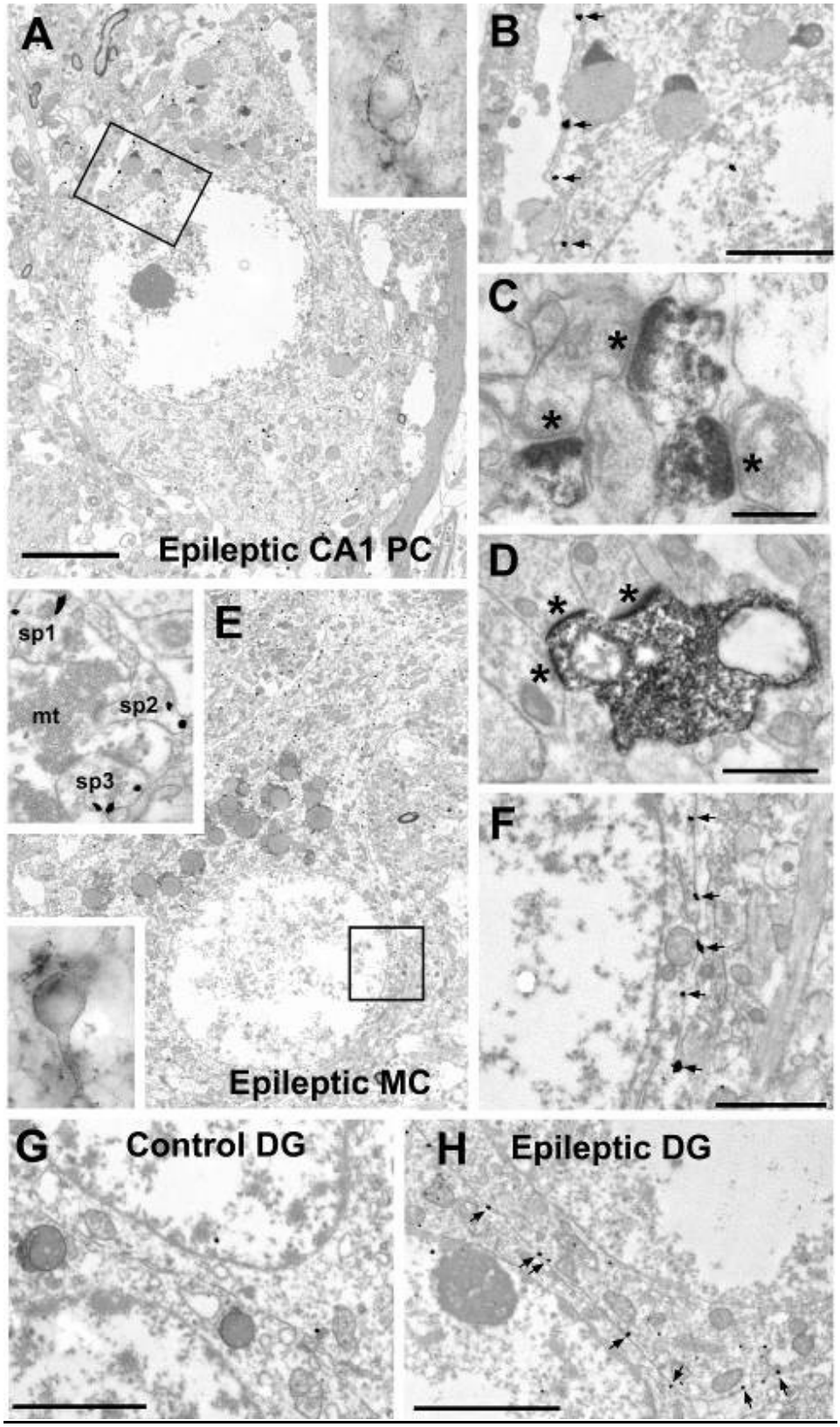
A
B
C
D
E
F
G
H
Epileptic CA1 PC
sp1
mt
sp2
sp3
Epileptic MC
Control DG
Epileptic DG

Figure 5: Electron micrographs show preembedding immunogold and DAB labelling of KCC2 in human tissue. Silver-enhanced gold particles signalling KCC2-immunopositivity are present on the membrane of CA1 pyramidal cell bodies of TLE patients (A and B, arrows); the same cell is shown at the light microscopic level in the upper right small insert in A. The framed area is shown at higher power in B. Spines of principal cells receiving asymmetric synaptic input were also intensively KCC2-immunoreactive (C, arrows), similarly to interneuron dendrites receiving multiple asymmetric synaptic contacts (asterisks) are shown in D. Mossy cell bodies (lower insert in E shows the same cell at the light microscopic level) and their dendrites and spines (see small upper insert, sp: spine, mt: mossy terminal) are also positive for KCC2 in epileptic samples. The framed area is shown at higher power in F, arrows point to the silver-enhanced gold particles. Granule cell bodies are negative for KCC2 in the control (G), whereas their dendrites and somata contain numerous silver-enhanced gold particles in the epileptic cases (H, small arrows). Asterisks indicate synapses. Scales: A,E: 5 µm; B,F: 2 µm; G,H: 2.5µm; C, D: 0.5µm

CA1: Cornu Ammonis region1, DG: Dentate Gyrus, KCC2: Type 2 potassium-chloride cotransporter, TLE: Temporal Lobe Epilepsy

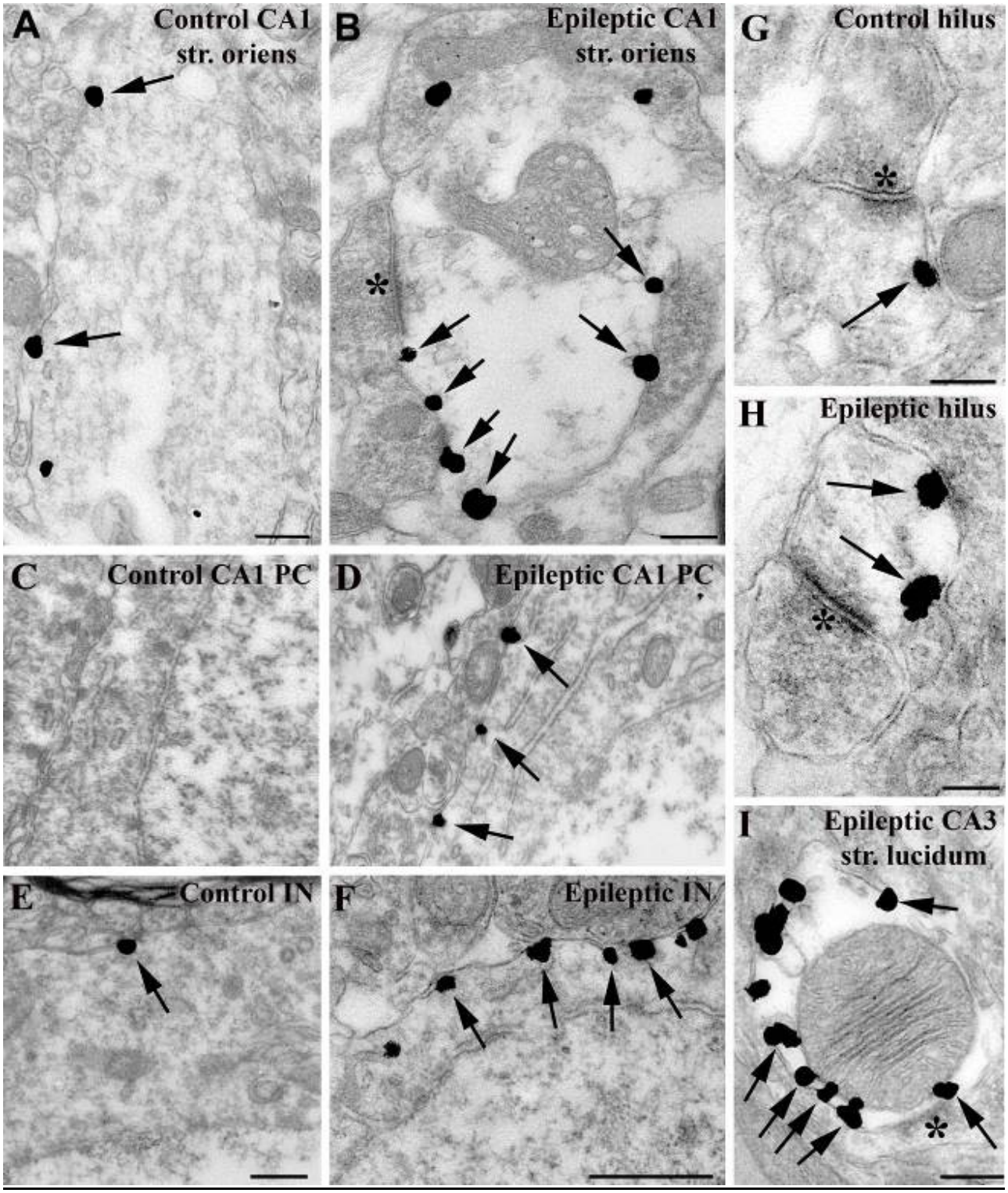

Figure 6: Electron micrographs show preembedding immunogold labelling of KCC2 in the mouse hippocampus. In control tissue silver-enhanced gold particles indicating KCC2-immunopositivity are present in the membrane of dendrites (A, arrows), and in dendritic spines

(G). Principal cell somata appear free of staining (C) whereas the cell body of interneurons may express KCC2 (see arrow in E). In epileptic tissue, the density of sliver-enhanced gold particles is increased in dendrites and dendritic spines (B,H,I). Principal cell somata become positive for KCC2 (D), and a strong upregulation of KCC2-expression can be seen in the membrane of certain interneurons (F). Silver-enhanced gold particles are usually present extrasynaptically, near asymmetric synapses (B,H and I). Asterisks indicate synapses. Scales: A, B and G-I: 0,2µm; C-F: 0,5µm

CA1: Cornu Ammonis region1, CA3: Cornu Ammonis region 3, DG: Dentate Gyrus, KCC2: Type 2 potassium-chloride cotransporter

Supplementary Material

Supplementary experimental procedures

Animal model of epilepsy

Based on the severity of acute seizures, animals were classified as weakly and strongly epileptic using a modified Racine's scale (Racine, 1972). Mice in the strongly epileptic group produced frequent, tonic-clonic seizures with intense motor symptoms (Racine 4-5), while members of the weakly epileptic group had rare and mild seizures (Racine 1-3) (Magloczky et al., 2010). In addition, chronic recurrent seizures were typical for strongly epileptic mice, and hardly ever found in members of the weakly epileptic group (Karlocai et al., 2011).

The acute phase was studied 30 minutes to 2 hours after the induction of seizures. The period examined 1-3 days after the injection was regarded as the latent phase. At day three post-injection, mass cell loss began in certain animals, therefore, this time point was considered as the end of the latent phase. At least 30 days after seizure induction we studied the chronic phase, when recurrent seizures could be observed (Karlocai et al., 2011).

Mice were perfused under equithesine anesthesia (chlornembutal 0.3 mL/100 g), first with physiological saline (3 min) and then with a fixative containing 0.05% glutaraldehyde, 4% paraformaldehyde and 15% picric acid in 0.1 M PB for 30 min.

Immunocytochemistry

60 µm thick vibratome sections were cut from the blocks, and following washing in PB, they were immersed in 30% sucrose for 1-2 days, then freeze-thawed three times over liquid nitrogen. Sections were processed for immunostaining as follows: after thorough washing in TRIS buffered saline (TBS, pH, 7.4) several times, endogenous peroxidase activity was blocked by 1% H_2O_2 in TBS for 10 minutes. TBS was used for all the washes (3x10 min between each antiserum) and for dilution of the antisera. Non-specific immunostaining was blocked by 5% milk powder and 2 % bovine serum albumin for human samples and 10% normal goat serum for mouse samples. To ensure that the stained elements are indeed specific for KCC2 two polyclonal rabbit KCC2 antisera were used for human tissue. The dilution of the first antibody was 1:500 (used only for human tissue) (Williams et al., 1999), whereas it was 1:10 000 for the second antibody (Rivera et al., 1999; Williams et al., 1999). Since the two antibodies showed exactly the same distribution of KCC2, the latter one was used for mouse tissue at a dilution of 1:10 000. For analysing cell loss, rabbit anti-GluR2/3 staining was also carried out (Chemicon International, 1:100) (not shown). For both KCC2 and GluR2/3 stainings, sections were incubated in the antisera for two days at 4^{o}C. For the visualization of the immunopositive elements, biotinylated anti-rabbit IgG (1:300, Vector) was applied as secondary serum followed by avidin-biotinylated horseradish peroxidase complex (ABC, 1:250, Vector). Sections were incubated for 20 minutes in 3,3'-Diaminobenzidine tetrahydrochloride (DAB, Sigma) as a chromogene dissolved in TRIS buffer (TB, pH=7.6) and the immunoperoxidase reaction was developed by 0.01% H_2O_2. Sections were then treated with 1% OsO_4 in 0.1 M PB for 40 min, dehydrated in ethanol (1% uranyl acetate was added at the 70% ethanol stage for 40 min) and mounted in Durcupan (ACM, Fluka).

A preembedding immunogold reaction was carried out in the same way, but after 48 h incubation in KCC2 primary antiserum, sections were washed extensively and blocked in 0.8% BSA, 0.1% IGGS gelatin (Amersham Life Science) and 5% normal goat serum in TBS for 30 min. This was followed by incubation with 1 nm gold-labelled goat anti-rabbit IgG (Amersham Life Science) diluted 1:50 in 0.8% BSA, 0.1% IGGS gelatin, 0.1 mg/ml glycine and lysine (Sigma) and 1% normal goat serum in TBS overnight. After incubation, sections were washed and postfixed with 1% glutaraldehyde in TBS for 10 min. The 1 nm gold particles were silver-

enhanced by IntenSE^{TM} M (Amersham Life Science) for 5-15 min. The sections were treated with 1% OsO_4 in 0.1 M PB for 10 min, and dehydrated in ascending ethanol series and embedded in Durcupan (ACM, Fluka). During dehydration, the sections were treated with 1% uranyl acetate in 70% ethanol for 30 min.

After light microscopic examination, areas of interest were re-embedded and sectioned for electron microscopy. Ultrathin serial sections were collected on Formvar-coated single slot grids, stained with lead citrate, and examined with a Hitachi 7100 electron microscope.

For light microscopic investigation of the KCC2-immunoreactive elements, 12 control and 32 epileptic human samples were used, whereas 19 control and 47 epileptic mouse hippocampi were chosen. For electron microscopic examination three controls and six epileptic human samples were taken, whereas five control and eight epileptic mouse hippocampi were analysed. All subfields of the control and epileptic hippocampi were examined in the electron microscope.

Western blot analysis

Preparation of crude membrane fractions: Human samples for sodium dodecyl sulphate containing polyacrylamide gel electrophoresis (SDS-PAGE) were prepared as follows: Tissue was weighed and homogenized in ice-cold lysis buffer: 25mM HEPES, 1mM EDTA, 6mM $MgCl_2$, 1mM Dithiothreitol (DTT), pH 7.4, supplemented with protease inhibitors (Complete, Roche) with a polytron homogenizer for 30 sec at maximum speed. The homogenate was adjusted to 10% (w/v) and centrifuged at 700xg for 5 min at 4°C to remove the nuclei. The supernatant was collected. The pellets were re-suspended in the original volume of lysis buffer, re-homogenized and spun down at 700xg for 5 min at 4°C. The supernatant containing the soluble proteins was collected and frozen for later analysis. The membrane pellets were re-suspended with a pipette using the original volume of lysis buffer and spun down as above. Supernatants were discarded, the pellets were resuspended in 1/30 of original volume lysis buffer, and the protein content was measured using the Bradford assay (Bradford, 1976).

Mouse samples for sodium dodecyl sulphate containing polyacrylamide gel electrophoresis (SDS-PAGE) were prepared as follows: Tissue was weighed and homogenized in ice-cold lysis buffer: 25mM HEPES, 1mM EDTA, 6mM $MgCl_2$, 1mM Dithiothreitol (DTT), pH 7.4, supplemented with protease inhibitors (Complete, Roche) with a homogenizer for 10

minutes. The homogenate was adjusted to 20% (w/v) and centrifuged at 700xg for 5 min at 4°C to remove the nuclei and debris. The supernatant was collected (S1). The pellets were re-suspended in half of the original volume of lysis buffer, re-homogenized and stored on ice for half an hour, then spun down at 700xg for 5 min at 4°C. The supernatant (S2) was collected. Supernatant fractions S1 and S2 were mixed and homogenized, then the protein content was measured using the Bradford assay (Bradford, 1976). Samples were stored frozen for later analysis.

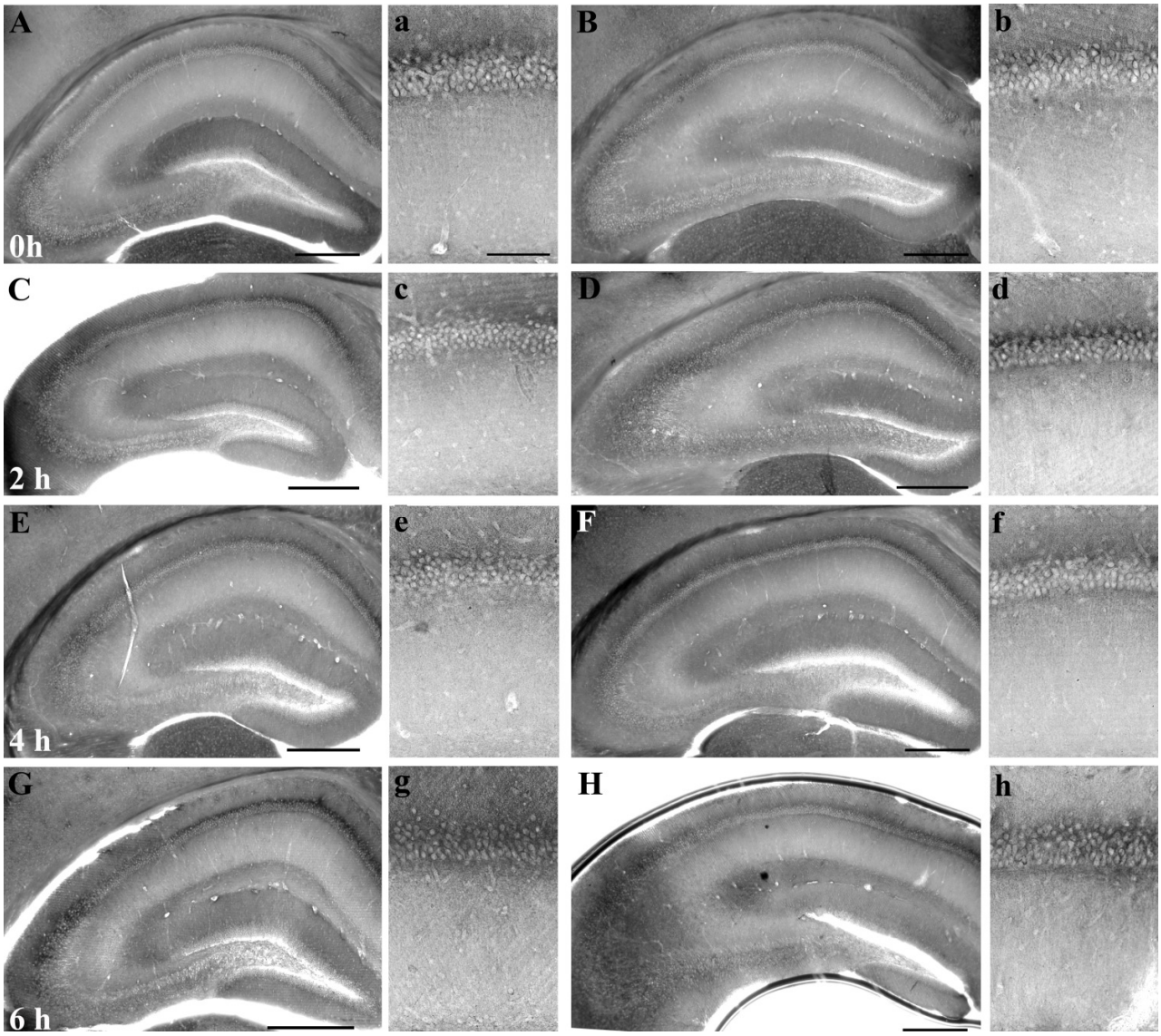

Supplementary Figure 1: The effect of post-mortem delay on KCC2-staining was examined in mice 0, 2, 4 and 6 hours after death (2 individuals each). No alteration was found after 0-4 hour post mortem delay (capital letters indicate entire hippocampi, whereas minuscule letters show region CA1 in greater magnification). In mice with 6 hours post mortem delay, a slight increase in intensity of KCC2 immunoreaction appeared, but the distribution of immunoreactive elements was similar at each time point. Scale: A-H: 500 µm, a: 100 µm.

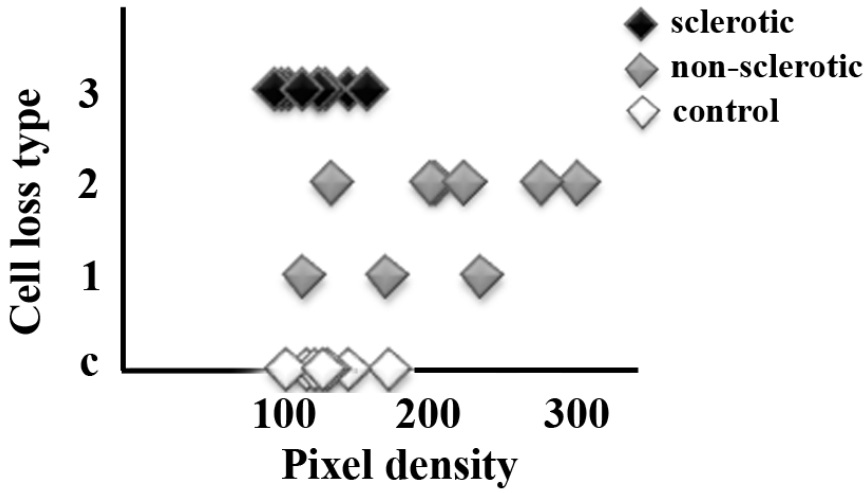

Supplementary Figure 2: Western blots were analysed calculating pixel densities. In non-sclerotic samples pixel density increased as a function of cell loss (largest in type 2 epileptic samples). However, in sclerotic samples pixel density only slightly differed from controls, due to intense cell loss.

Supplementary References

Bradford, M.M. 1976. A rapid and sensitive method for the quantitation of microgram quantities of protein utilizing the principle of protein-dye binding. *Anal Biochem*. 72:248-254.

Karlocai, M.R., K. Toth, M. Watanabe, C. Ledent, G. Juhasz, T.F. Freund, and Z. Magloczky. 2011. Redistribution of CB1 cannabinoid receptors in the acute and chronic phases of pilocarpine-induced epilepsy. *PloS one*. 6:e27196.

Magloczky, Z., K. Toth, R. Karlocai, S. Nagy, L. Eross, S. Czirjak, J. Vajda, G. Rasonyi, A. Kelemen, V. Juhos, P. Halasz, K. Mackie, and T.F. Freund. 2010. Dynamic changes of CB1-receptor expression in hippocampi of epileptic mice and humans. *Epilepsia*. 51 Suppl 3:115-120.

Racine, R.J. 1972. Modification of seizure activity by electrical stimulation: II. Motor seizure. *Electroencephalography and clinical neurophysiology*. 32:281-294.

Rivera, C., J. Voipio, J.A. Payne, E. Ruusuvuori, H. Lahtinen, K. Lamsa, U. Pirvola, M. Saarma, and K. Kaila. 1999. The K+/Cl- co-transporter KCC2 renders GABA hyperpolarizing during neuronal maturation. *Nature*. 397:251-255.

Williams, J.R., J.W. Sharp, V.G. Kumari, M. Wilson, and J.A. Payne. 1999. The neuron-specific K-Cl cotransporter, KCC2. Antibody development and initial characterization of the protein. *J Biol Chem*. 274:12656-12664.